Citation: Molecular Therapy—Nucleic Acids (2016) 5, e389; doi:10.1038/mtna.2016.92
Official journal of the American Society of Gene & Cell Therapy
www.nature.com/mtna

In vivo Editing of the Human Mutant *Rhodopsin* Gene by Electroporation of Plasmid-based CRISPR/Cas9 in the Mouse Retina

Maria Carmela Latella[1], Maria Teresa Di Salvo[2], Fabienne Cocchiarella[1], Daniela Benati[1], Giulia Grisendi[3], Antonella Comitato[2], Valeria Marigo[2] and Alessandra Recchia[1]

The bacterial CRISPR/Cas system has proven to be an efficient tool for genetic manipulation in various organisms. Here we show the application of CRISPR-Cas9 technology to edit the human *Rhodopsin* (*RHO*) gene in a mouse model for autosomal dominant Retinitis Pigmentosa. We designed single or double sgRNAs to knock-down mutant *RHO* expression by targeting exon 1 of the *RHO* gene carrying the P23H dominant mutation. By delivering Cas9 and sgRNAs in a single plasmid we induced an efficient gene editing *in vitro*, in HeLa cells engineered to constitutively express the P23H mutant *RHO* allele. Similarly, after subretinal electroporation of the CRISPR/Cas9 plasmid expressing two sgRNAs into P23H *RHO* transgenic mice, we scored specific gene editing as well as significant reduction of the mutant RHO protein. Successful *in vivo* application of the CRISPR/Cas9 system confirms its efficacy as a genetic engineering tool in photoreceptor cells.

Molecular Therapy—Nucleic Acids (2016) **5**, e389; doi:10.1038/mtna.2016.92; published online 22 November 2016
Subject Category: Gene Insertion, Deletion & Modification

Introduction

G-protein coupled receptors (GPCR) are receptors for hormones, neurotransmitters, drugs, and sensory stimuli that play key roles in cellular metabolism and activity.[1] Point mutations in GPCR often cause protein misfolding and endoplasmic reticulum (ER)-retention associated with pathological conditions.[2] *Rhodopsin* (*RHO*) is one of the best characterized GPCR specifically expressed by rod photoreceptor cells and is composed by a protein opsin and a chromophore, 11-*cis* retinal. Photon absorption, inducing *cis*–*trans* isomerization of 11-*cis* retinal, triggers the phototransduction cascade required for vision. Dominant mutations in *RHO* represent a common cause of Retinitis Pigmentosa (RP), accounting for 25% of autosomal dominant RP and 8 to 10% of all RP[3] with over 140 different mutations identified so far (http://www.hgmd.cf.ac.uk). The majority of the biochemically characterized RHO mutants are likely misfolded and retained into the ER with a pathogenic mechanism well studied but still not fully characterized.[4–8] RP is an inherited form of retina degeneration leading to blindness with patients experiencing progressive loss of the peripheral field and, at later stages, compromising also the central part of the retina. Studies in transgenic mice bearing dominant *RHO* mutations showed that disease severity could be mitigated by transcriptional suppression using an allele-independent approach to target both mutant and wild-type alleles.[9] Botta *et al.*[10] recently showed the efficacy of *RHO* transcriptional repression mediated by artificial zinc finger proteins without canonical effector domain in pig retinas. Coupled to DNA-binding-mediated silencing, they provided human *RHO* cDNA to complement *RHO* transcriptional repression demonstrating the therapeutic potential of the combined silencing-replacement strategy in a large animal model.

Another strategy to tackle the autosomal dominant RP mutations spread all along the transcription unit is a mutation-independent knock-out of the *RHO* gene. This approach requires, as for the *RHO* transcriptional silencing, a combined replacement therapy with a wild type *RHO* gene.[11] Genetic perturbation mediated by the clustered regularly interspaced short palindromic repeat (CRISPR)-CRISPR-associated protein 9 (Cas9) provides an alternative approach for gene silencing. The CRISPR-Cas system[12,13] has been shown to have enormous potential for gene editing in a variety of hosts such as plants,[14] zebrafish,[15] flies,[16] mice,[17] monkeys,[18] and also in human cells.[19–21] The type 2 CRISPR/Cas9 system induces DNA double strand breaks (DSBs). The DSBs can stimulate cell repair mechanisms including nonhomologous end joining (NHEJ) and homology-directed repair (HR), but in most circumstances, NHEJ is the predominant mechanism for repairing DSBs. Small insertions and deletions created by NHEJ DNA repair can be used to generate frameshifts to abolish the expression of mutant alleles.[22]

In this study, we addressed the efficacy of the CRISPR/Cas9 system in rod photoreceptors to selectively generate loss-of-function mutations in the first exon of human *RHO* gene resulting in robust knock-down of *RHO* expression *in vitro* and *in vivo,* in the available P23H transgenic mouse

The first two authors contributed equally to this work.
[1]Department of Life Sciences, Centre for Regenerative Medicine, University of Modena and Reggio Emilia, Modena, Italy; [2]Department of Life Sciences, University of Modena and Reggio Emilia, Modena, Italy; [3]Department of Medical and Surgical Sciences for Children & Adults, Laboratory of Cellular Therapies, University Hospital of Modena and Reggio Emilia, Modena, Italy Correspondence: Alessandra Recchia, Department of Life Sciences, Centre for Regenerative Medicine, University of Modena and Reggio Emilia, Modena, Italy. E-mail: alessandra.recchia@unimore.it or Valeria Marigo, Department of Life Sciences, University of Modena and Reggio Emilia, Modena, Italy. E-mail: valeria.marigo@unimore.it
Keywords: Human Rhodopsin; CRISPR/SpCas9 plasmids; in vivo gene editing
Received 12 August 2016; accepted 1 September 2016; published online 22 November 2016. doi:10.1038/mtna.2016.92

model for RP bearing a human P23H mutant *RHO* minigene. Since no human cell line constitutively expressing *RHO* (normal or mutated) is available, we developed an *in vitro* cell-based system to test the CRISPR activity by engineering HeLa cells to constitutively express either wild type or mutant P23H *RHO*. We compared efficiencies at genomic, transcriptional, and protein levels *in vitro* and in rod cells *in vivo* of single versus double-combined single-guide RNAs (sgRNAs). An almost complete clearance of RHO expression *in vitro* and a strong reduction of human RHO *in vivo* were achieved combining two sgRNAs in a single effector plasmid. Editing analysis of predicted off-target sites by Cel-I assay did not detect mutations with frequencies ≥ 1%. Therefore, CRISPR/Cas9 disruption of *RHO* provides an excellent gene modification tool for future knock-out or therapeutic applications in the retina.

Results

Genome editing of the human *RHO* gene

To employ the *CRISPR/Cas9* gene editing platform for correcting a wide range of *RHO* mutations, we created a couple of sgRNAs tailored to exon 1 of the *RHO* gene in order to abolish the expression of the vast majority of dominant mutations spread all along the transcription unit of *RHO*.[23] We employed the previously described *Staphylococcus pyogenes* nuclease that utilizes a human-codon optimized SpCas9[19,24] and a chimeric sgRNA expression vector to direct efficient site-specific gene editing. We designed two protospacers in opposite DNA strands and in a tail-to-tail configuration meeting the 5′-NGG-3′ PAM requirement of SpCas9 to target exon 1 (**Figure 1**). Small insertions or deletions created by NHEJ-based DNA repair within this exon can generate frameshift mutations within the selected protospacers knocking out *RHO*. The PAM sequence, 5′-GGG-3′, is recognized by sgRNA3, whereas sgRNA1, in reverse orientation, targets the PAM 5′-TGG-3′ present in the P23H mutant allele. The sgRNAs were intentionally targeted in the region with the single nucleotide C to A (nt 68 from ATG) conversion accounting for the P23H *RHO* mutation that represents our experimental *in vitro* and *in vivo* models. Although the PAM 5′-TGG-3′ is present only in the P23H allele, sgRNA1 could recognize the PAM 5′-GGG-3′ present in the wild type allele. Thereby, none of the two sgRNAs are mutation specific. The sgRNAs were cloned in the pX330 backbone to generate sgRNA1, sgRNA3, and 2sgRNA plasmids (see **Supplementary Figure S1**).

In vitro knock-down of mutant *RHO* expression by targeted gene editing

We created HeLa cell lines stably expressing P23H-*RHO* because no cell line expressing *RHO* was available and thus mRNA and protein analyses could not be assessed after genome editing. To assess the *RHO* gene knock-down *in vitro* we generated HeLa stable clones using lentiviral vectors encoding the mutant P23H-*RHO* cDNA under the phosphoglycerate kinase (PGK) promoter. Basically, we transduced HeLa cells at low multiplicity of infection to favor the integration of few copies of lentivirus per cell and found ~20% of the cells producing RHO protein as detected by immunofluorescence analysis (data not shown). We cloned the bulk population by limiting dilution to isolate 34 clones showing a stable integration of the lentiviral vector. We determined the relative vector copy number (VCN) of the mutated *RHO* transgene in each clone by quantitative polymerase chain reaction (qPCR) (see **Supplementary Figure S2a**). We selected two clones (#78 and #80) harboring two and one copy, respectively, and investigated the subcellular distribution of mutant RHO protein by immunofluorescence analysis. We expected no plasma membrane localization and ER retention of the mutant protein.[25,26] In both clones P23H RHO protein could not be detected at the plasma membrane (see **Supplementary Figure S3**) but its localization was intracellular in the ER as defined by the colocalization with the ER-resident chaperone calnexin[27] (see **Supplementary Figure S4a**). On the contrary, two HeLa clones (#42 and #73) harboring two copies each of a lentiviral vector expressing wild type *RHO* under the PGK promoter (see **Supplementary Figure S2b**) showed membrane localization (see **Supplementary Figure S3**) and limited colocalization with calnexin (see **Supplementary Figure S5**) confirming

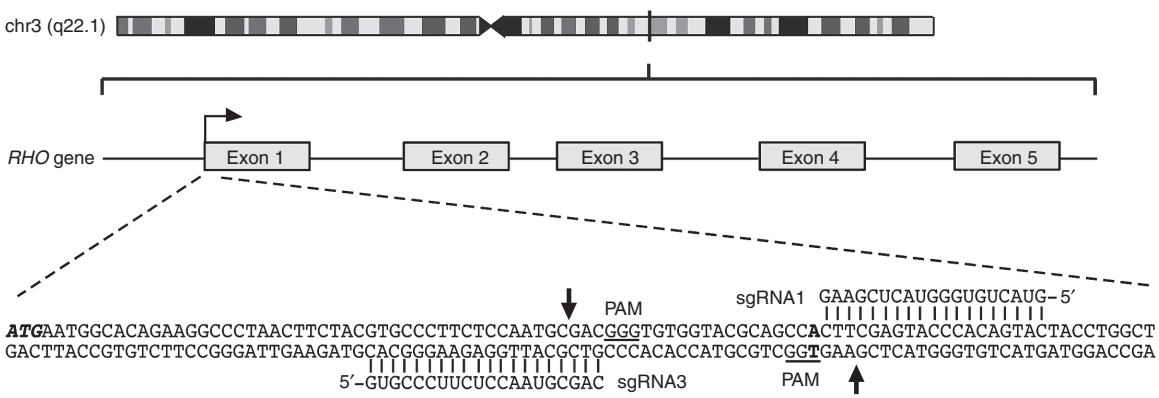

Figure 1 CRISPR/Cas9 targeting of the human *RHO* gene. Schematic representation of human chromosome 3 and *RHO* gene. The magnified view illustrates the sgRNAs and the PAM sequences (underlined) tailored to exon 1. The C to A conversion resulting in the P23H mutation present in the first exon of the *RHO* gene is highlighted in bold. Start codon of *RHO* gene is in italic. Black arrowheads indicate cleavage sites.

that the selected clones can be an appropriate *in vitro* model displaying a proper expression of wild type and P23H mutant *RHO*. We quantified the colocalization of RHO and calnexin by measuring the Pearson Correlation Coefficient (PCC)[28] and found a significantly higher ER retention and consequently higher PCC of P23H mutant RHO when compared with wild type (see **Supplementary Figure S4b**). Both clones expressing P23H behaved similarly, all experiments from now on were performed on clone #78 showing higher P23H *RHO* expression (see **Supplementary Figure S6**).

We initially assessed frequency of gene editing in the P23H HeLa clone #78 2 days post-transfection by the Surveyor assay. We found that tested sgRNAs, either single or in couple in a single plasmid (2sgRNA) when coexpressed with the SpCas9 nuclease were able to mediate gene modification on the PGK-driven *RHO* expression cassette (**Figure 2a**). Notably, HeLa cells transfected with the 2sgRNA plasmid and not treated with Cel I nuclease resulted in a full-length (FL) and in short-edited (SE) amplicons confirming the expected deletion of the region between the two selected protospacers (SE in **Figure 2a**). Using specific primers recognizing the endogenous wild type locus of *RHO* we defined, as expected, that both sgRNAs are not mutation specific (data not shown).

The frequency of Indels in the P23H clone transfected with sgRNA1, sgRNA3, and 2sgRNA were measured by sequencing 130 PCR amplicons encompassing the target sites and resulted in 70, 76, and 82% Indels respectively (**Table 1**). The types of insertions and deletions generated by sgRNA1, sgRNA3, and 2sgRNA at this locus showed variable patterns of rearrangements of the coding sequence, insertion of up to 3 nt and deletion from 1 to 91 nucleotides (**Figure 2b**). Deletion of region between the 2 PAMs was observed in the cells transfected with 2sgRNA plasmid. These deletions were also observed at mRNA level by reverse-transcriptase (RT)-PCR flanking the Cas9 target site on exon 1. Indeed a FL and SE P23H mRNAs were observed in the 2sgRNA treated clone. Conversely, the RT-PCR analysis performed on mRNA extracted from P23H HeLa clone transfected with sgRNA1 and sgRNA3 did not show SE bands (**Figure 3a**). However in all CRISPR/Cas9 treated samples we observed a reduction of *RHO* expression compared with the untransfected or pX330-transfected cells (**Figure 3a**). We quantified this reduction by Real time Taqman PCR and found a significant knock-down of *RHO* expression in samples exposed to sgRNA1, sgRNA3, and 2sgRNA plasmids (35, 25, 20%, respectively) (**Figure 3b**).

Finally, we evaluated the RHO protein production by immunoblotting on total protein extracts from P23H HeLa clone #78 transfected with sgRNA1, sgRNA3, and 2sgRNA (**Figure 3c**). We observed a strong reduction upon transfection with single sgRNAs or 2sgRNA, respect to untransfected cells. Based on genomic, transcriptomic, and protein results we selected 2sgRNA for the *in vivo* experiments.

Off-targets and cytotoxicity analyses

Before embarking in the *in vivo* experiments, we assessed the cytotoxicity and the off-targets of the designed sgRNAs in our *in vitro* model. Induction of apoptosis in CRISPR/Cas9-expressing cells was evaluated by labelling transfected HeLa clone #78 with 7-aminoactinomycin D (7-AAD) in combination with PE-Annexin V. This flow-cytometry-based assay allowed the discrimination of early apoptotic cells (AnnexinV$^+$/7-AAD$^-$) and late apoptotic/necrotic cells (7-AAD$^+$). P23H HeLa clone #78 was transfected with a plasmid coding only for Cas9 fused to a GFP reporter (pL.CRISPR-GFP) and similar plasmids bearing also the sgRNAs employed in this study (pL.CRISPR-GFP.sgRNA1, pL.CRISPR-GFP.sgRNA3, and pL.CRISPR-GFP.2sgRNA). As control we transfected a plasmid coding only for the GFP reporter (pPGK.GFP). Cytotoxicity analysis was performed on the GFP$^+$ subpopulation scored in all samples. Similar profiles of early or late apoptotic/necrotic cells were observed in all samples with minimal induction of apoptosis in transfected cells (8–12% of early apoptotic cells and <10% of late apoptotic/necrotic cells) without significant differences among samples (analysis of variance (ANOVA), $P \leq 0.01$) (see **Supplementary Figure S7**). These results proved no toxicity associate to the expression of the CRISPR/Cas9 system in human cells.

To predict the most likely off-target sites for the sgRNAs used to knock-down the *RHO* gene in this study, we used a public webserver (http://crispr.mit.edu) able to assess and prioritize potential CRISPR/Cas9 activity at off-target loci based on predicted positional bias of a given mismatch in the sgRNA protospacer sequence and the total number of mismatches to the intended target site.

The CRISPR design tool scored a total of 201 (111 for sgRNA1 and 90 for sgRNA3) potential off-target sites in the human genome and were listed in **Supplementary Table S1a,b** the top 20 off targets with a score ≥ 0.2. The top five potential off-target sites ($0.4 \leq$ score ≤ 0.7) for each sgRNA were assessed by the Surveyor assay in the P23H HeLa clone #78 edited with a high frequency (**Table 1**). None of the 10 predicted off-target loci had significant levels of off-target gene modification detectable by Cel I assay (**Figure 4a**,**b** and **Supplementary Table S1**).

Specific editing of human *RHO* in the P23H transgenic mouse model

To demonstrate the ability of the CRISPR/Cas9 system to edit the human *RHO* gene in the retina *in vivo*, we availed of a transgenic mouse model carrying the human P23H mutant alleles.[29] To better characterize expression of the human P23H-*RHO* transgene without interference by the murine *Rho* gene we bred the mice with *Rho*$^{-/-}$ knock-out mice[30] and generated mice expressing only the human P23H mutant *RHO* (*Rho*$^{-/-}$P23H^{Tg}). We electroporated the 2sgRNA plasmid together with a plasmid expressing GFP to track the transfected cells in the retina. Electroporation was performed after subretinal injection as previously published.[31,32] We evaluated expression of Cas9 in the electroporated retinas after dissection of the GFP$^+$ area (**Figure 5a**) and found a specific expression in the electroporated left eye that strongly correlated with expression of GFP (**Figure 5b**). These data allowed us to be confident that GFP$^+$ cells were also expressing Cas9. We thus fluorescence-activated cell sorting (FACS)-sorted electroporated retinal cells based on GFP expression. We firstly confirmed the presence of photoreceptor cells in the negative and positive fractions by RT-PCR by analysis of *Pde6b* expression, a gene expressed only in rod photoreceptors (**Figure 6a**), and then

a

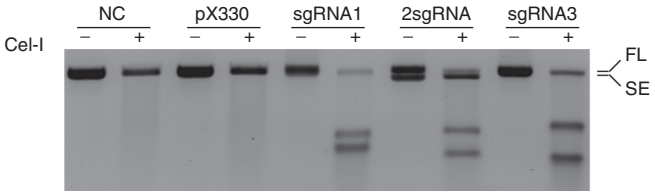

b

sgRNA1

Deletions

```
CGGGTGTGGTACGCAGCCACTTCGAGTACCCACAGTACTACCTGGCTGAGCC (x13) Lenght
CGGGTGTGGTACGCAGC-------AGTACCCACAGTACTACCTGGCTGAGCC       -7
CGGGTGTGGTACGCAGCCACTT--------TACAGTACTACCTGGCTGAGCC (x2)  -8
CGGGTGTGGTACGCAGCCACTT----TACCCACAGTACTACCTGGCTGAGCC       -4
CGGGTGTGGTACGCAGCCACTT---TTACCCACAGTACTACCTGGCTGAGCC       -3
CGGGTGTGGTACGCAGCCACTTC--TTACCCACAGTACTACCTGGCTGAGCC (x2)  -2
CGGGTGTGGTACGCAGCCACTT-GAGTACCCACAGTACTACCTGGCTGAGCC       -1
CGGGTGTGGTACGCAGCCAC-------------AGTACTACCTGGCTGAGCC (x2)  -13
CGGGTGTGGTACGCAGCCACT-GTGGTACCCACAGTACTACCTGGCTGAGCC       -1
CGGGTG-----------------------------------------GCTGAGCC       -38
CGGGTGTGGTA-----------CGAGTACCCACAGTACTACCTGGCTGAGCC       -11
CGGGTG----------------CGAGTACCCACAGTACTACCTGGCTGAGCC       -16
CGGGTGTGGTACGCAGCCACT---------------ACTACCTGGCTGAGCC       -15
CGGGTGTGGTACGCAGCCACTT-TAGTACCCACAGTACTACCTGGCTGAGCC       -1
CGGGTG-----------------------------------CGTGGTGAGCC       -35
CGGGTGTGGTACGCAGCCACTT-GAGTACCCACAGTACTACCTGGCTGAGCC       -1
CGGGTG------------------------------------------AGCC       -42
CGGGTGTGGTACGCAGCCACTT--------------ACTACCTGGCTGAGCC       -14
CGGGTGTGGTACGC---------GAGTACCCACAGTACTACCTGGCTGGGCC       -9
CGGGTGTGGTACGCAGCCAC----AGTACCCACAGTACTACCTGGCTGAGCC       -4
CGGGTGTGGTACGCAGCCACT-CGAGTACCCACAGTACTACCTGGCTGAGCC       -1
CGGGTGTGGTACGCAGCCACTT--AGTACCCACAGTACTACCTGGCTGAGCC       -2
CGGGTGTGGTACGCAGCCACTTC-----------GTACTACCTGGCTGAGCC       -11
CGGGTGTGGTAC-----------------------------------------       -91
```

Insertions

```
CGGGTGTGGTACGCAGCCACTT---CGAGTACCCACAGTACTACCTGGCTGA
CGGGTGTGGTACGCAGCCACTTCGACGAGTACCCACAGTACTACCTGGCTGA (x2)  +3
CGGGTGTGGTACGCAGCCACTTC--CGAGTACCCACAGTACTACCTGGCTGA       +1
CGGGTGTGGTACGCAGCCACTTT--CGAGTACCCACAGTACTACCTGGCTGA       +1
```

sgRNA3

Deletions

```
TTCTACGTGCCCTTCTCCAATGCGACGGGTGTGGTACGCAGCCACTTCGAG  (x10) Lenght
TTCTACGTGCCCTTCTCTAATGC-ACGGGTGTGGTACGCAGCCACTTCGAG  (x3) -1
TTCTACGTGCCCTTCTCCAATG--ACGGGTGTGGTACGCAGCCACTTCGAG  (x5) -2
TTCTACGTGCCCTTC-----------------GTACGCAGCCACTTCGAG       -18
TTCTACGTGCCCTTCTC------GACGGGTGTGGTACGCAGCCACTTCGAG       -6
TTCTACGTGCCCTTCTCCAATGC-------CTGGTACGCAGCCACTTCGAG       -7
TTCTACGTGC----------------------------------TTCGAG       -35
TTCTACGTGCCCTTCTCCAATG-----GGTGTGGTACGCAGCCACTTCGAG       -5
TTCTACGTGCCCTTCT-------GACGGGTGTGGTACGCAGCCACTTCGAG       -7
TTCTACGTGCCCTTCTCCAGTG-------TGTACGCAGCCACTTCTTCGAG       -7
TTCTACGTGCCCTTCTCCAA--AGACGGGTGTGGTACGCAGCCACTTCGAG       -2
TTCTACGTGCCCTTCTCC-----GACGGGTGTGGTACGCAGCCCCTTCGAG       -5
TTCTACGTGCCCTTCTCCAATG-CGTTGGTGTGGTACGCAGCCACTTCGAG       -1
TTCTACGTGCCCTTCTCC-----GACGGGTGTGGTACGCAGCCCCTTCGAG       -5
TTCTACG-------------------------------CAGCCACTTCGAG       -31
```

Insertions

```
TTCTACGTGCCCTTCTCCAATGC-GACGGGTGTGGTACGCAGCCACTTCG
TTCTACGTGCCCTTCTCCAATGCCGACGGGTGTGGTACGCAGCCACTTCG  (x12) +1
```

2sgRNA

Deletions

```
TCCAATGCGACGGGTGTGGTACGCAGCCACTTCGAGTACCCACAGTAC    (x8) Lenght
TCCAATGC-----------------------CGAGTACCCACAGTAC    (x29) -24
TCCAATG------------------------CGAGTACCCACAGTAC    (x8)  -25
```

Figure 2 NHEJ-mediated knock-out of human *RHO* gene using the CRISPR/Cas9 system. (**a**) The Surveyor (Cel-I) nuclease assay on exon 1 of P23H *RHO* showed targeted cleavage of the digested PCR products in P23H HeLa clone #78 transfected with sgRNA1, sgRNA3, 2sgRNA but not with pX330 (no sgRNA) or in untransfected cells (negative control, NC; full-length, FL; short-edited, SE). Cells transfected with 2sgRNA show the short edited PCR product. (**b**) Sequence analysis of PCR products surrounding the Cas9 target sites in the genome of HeLa clone #78 transfected with sgRNA1, sgRNA3, and 2sgRNA (in bold) showed a wide variety of Indel mutations mediated by NHEJ at the targeted exon 1. The top sequence in red is the unmodified sequence, underlined are the PAMs. The mismatches/insertions are indicated in cyan. The number of PCR amplicons for each sequence is indicated in parentheses and the modified length is indicated.

Table 1 Gene editing frequency and Indels in P23H HeLa clone #78 transfected with sgRNA1, sgRNA3, and 2sgRNA

	sgRNA1		*sgRNA3*		*2sgRNA*	
	Number of edited sequences/total sequences	Frequency of InDels (%)	Number of edited sequences/ total sequences	Frequency of InDels (%)	Number of edited sequences/total sequences	Frequency of InDels (%)
Editing	30/43	70	32/42	76	37/45	82
Deletions	26/43	61	20/42	48	37/45	82
Insertions	4/43	9	12/42	28	–	–

Genomic DNAs of transfected cells were PCR-amplified with primers surrounding the targets sites. PCR products were cloned into PCR2.1 TOPO vector and sequenced. We analyzed the Indels in 43, 42, and 45 sequences for sgRNA1, sgRNA3, and 2sgRNA transfected cells respectively.

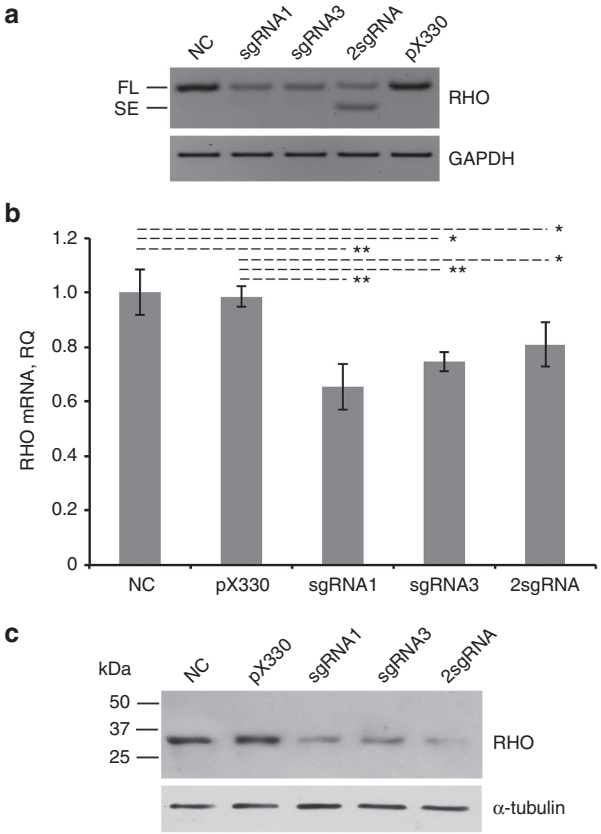

Figure 3 *In vitro* knock-down of human P23H RHO expression. (**a**) RT-PCR analysis on *RHO* expression in P23H HeLa clone #78 transfected with pX330, sgRNA1, sgRNA3, and 2sgRNA and untransfected cells (negative control, NC). FL indicates the full-length transcript. SE indicates the short edited transcript. RT-PCR was normalized by analysis of *GAPDH*. (**b**) Real time TaqMan PCR on *RHO* expression in untransfected P23H HeLa clone #78 (NC) or transfected with sgRNA1, sgRNA3, 2sgRNA, and pX330. The experiment was performed in triplicate and is presented as mean ± SEM (**P*-value < 0.05, ***P* < 0.01). (**c**) Western blottings on total protein extracts to analyse *RHO* expression in untransfected (NC, negative control) and nuclease-treated P23H HeLa clone #78. The 35 kDa monomer RHO protein is strongly reduced after exposure to sgRNA1, sgRNA3, and 2sgRNA but not after exposure to the control pX330. The western blotting was normalized using anti-α-tubulin antibodies (lower panel). GAPDH, glyceraldehyde 3-phosphate dehydrogenase.

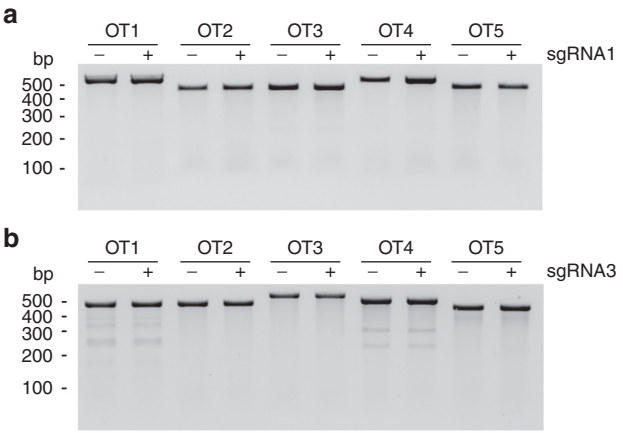

Figure 4 Evaluation of CRISPR/Cas9 off-target effects for sgRNAs designed to knock-down the human *RHO* gene. (**a**) and (**b**) Surveyor analysis at the top five potential off-target sites for sgRNA1 or sgRNA3 in P23H HeLa clone #78 transfected with pX330 (–) or with the corresponding sgRNA1 or 3 (+). OT: off-target locus.

we evaluated genome editing in both fractions. GFP⁻ cells did not show Indels (see **Supplementary Figure S8**) confirming that Cas9 expression was restricted to GFP⁺ cells, on the contrary 4–33% editing, was scored in GFP⁺ cells derived from 9 out 10 2sgRNA-treated retinas (**Table 2**). Specifically, Sanger sequencing of PCR amplicons ($n = 404$) surrounding the Cas9 target site of human P23H *RHO* gene edited in all 2sgRNA-treated mice, showed 84 edited sequences (21%), in particular 16% display the 24bp-deletion, 1% the inversion (insertion) of the sequence between the cleavage sites and 4% deletions of 5–25bp (**Figure 6b**). No sign of genome editing was observed on the human P23H *RHO* gene in retinas injected with pX330 plasmid (see **Supplementary Figure S9**) or on the mouse *Rho* gene in retinas treated with 2sgRNA (**Supplementary Figure S10**) indicating a human allele-specific Cas9-mediated genome editing. To address the knock-down efficiency on P23H *RHO* expression we performed a human *RHO* specific RT-PCR on GFP⁺ and GFP⁻ cells sorted from the 2sgRNA- and pX330-injected retinas. All the GFP⁺ retinal cells from the 2sgRNA-injected eyes showed the presence of the SE band corresponding to the deletions occurred on exon 1 of human *RHO* (**Figure 6c**). The ratio between the SE P23H bands to the unmodified one FL in the same sample was analyzed and ranged between 12–35% (see **Supplementary Figure S11** and **Table 2**). Finally, we wanted to define if targeting of the human *RHO* gene resulted in a reduction of RHO protein. To this aim, based on GFP expression, we cut the electroporated areas of four different

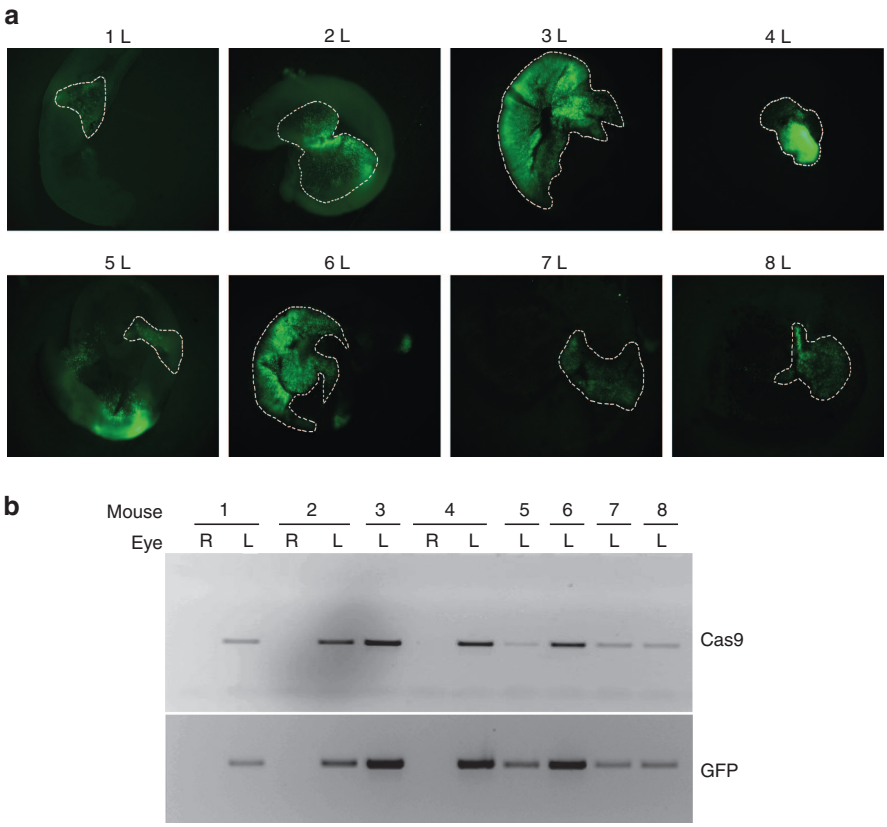

Figure 5 Electroporation of the CRISPR/Cas9 plasmids into mice retinas. (**a**) Microphotographs of electroporated retinas showing transfected areas labelled by GFP expression (green). Positive areas were cut at the stereoscope (dashed lines) and used for further analyses shown in **b**. (**b**) RT-PCR analysis on *Cas9* and *GFP* expression in eight mouse retinas injected with sgRNA1 (left eye, L). Mice 1, 2, and 4 show also expression analyses in the not injected contralateral (right, R) retinas. No expression of *Cas9* as well as *GFP* was detectable in these samples.

retinas transfected with the 2sgRNA plasmid and the electroporated areas of four different retinas transfected with the pX330 control plasmid and compared RHO protein amounts by western blotting (**Figure 6d**). All samples transfected with 2sgRNA showed significant decrease of RHO protein but no significant change was observed in samples transfected with pX330 (**Supplementary Figure S12a,b** and **Table 2**).

Discussion

In this study, we report the first *in vivo* CRISPR-Cas9-mediated editing of the human *RHO* gene carrying the Pro-23His dominant mutation associated with autosomal dominant RP.[33] Differentially from Bakondi *et al.*[34] that targeted the dominant murine S334ter mutation (*Rho*S334) in a rat model for severe autosomal dominant RP, we developed a mutation-independent editing approach tailored to human *RHO*. Gene correction of dominant mutations can be tackled by replacement of the mutation/s through homologous recombination with a portion of the wild type gene or by knocking-out the mutated allele followed by addition of the wild type coding sequence. Herein, we reported the feasibility of the CRISPR/Cas9 system to knock-down the human *RHO* gene *in vivo* in the P23H transgenic mouse model for RP.[29] This is a well-characterized animal model for RP generated with a human minigene derived from a patient. This animal model is characterized by intracellular protein accumulation and by a very fast retinal degeneration.[8,29] The presence of the human gene allowed us to test gene editing in photoreceptor cells *in vivo*. A limitation was the fast progression of photoreceptor cell demise in the absence of the endogenous *Rho* in this model that hampered functional studies that require retinas at older ages than the time points analyzed in this study.

A primary advantage of the knock-out approach is that NHEJ is an active DNA repair mechanism in all cell types, whereas homologous recombination is typically only active in mitotic cells, thus strongly disfavored in neurons like photoreceptors.[35] Another advantage of this approach is the possibility to generate two DSBs resulting in the precise excision of a short DNA fragment between two Cas9-mediated cleavage sites occurring 3 bp upstream each PAM sequence.[13] Thus, the protein product of the edited gene is predictable. This is in contrast to the random Indels created by intraexonic action of a single nuclease or by double nickase strategies based on D10-SpCas9 that will lead to the creation of novel proteins from each DNA repair event.

RHO-specific knock-out was achieved in 70–82% of the *RHO* mutant alleles carried by HeLa cells transfected with single or double sgRNAs respectively. Among the 82% of

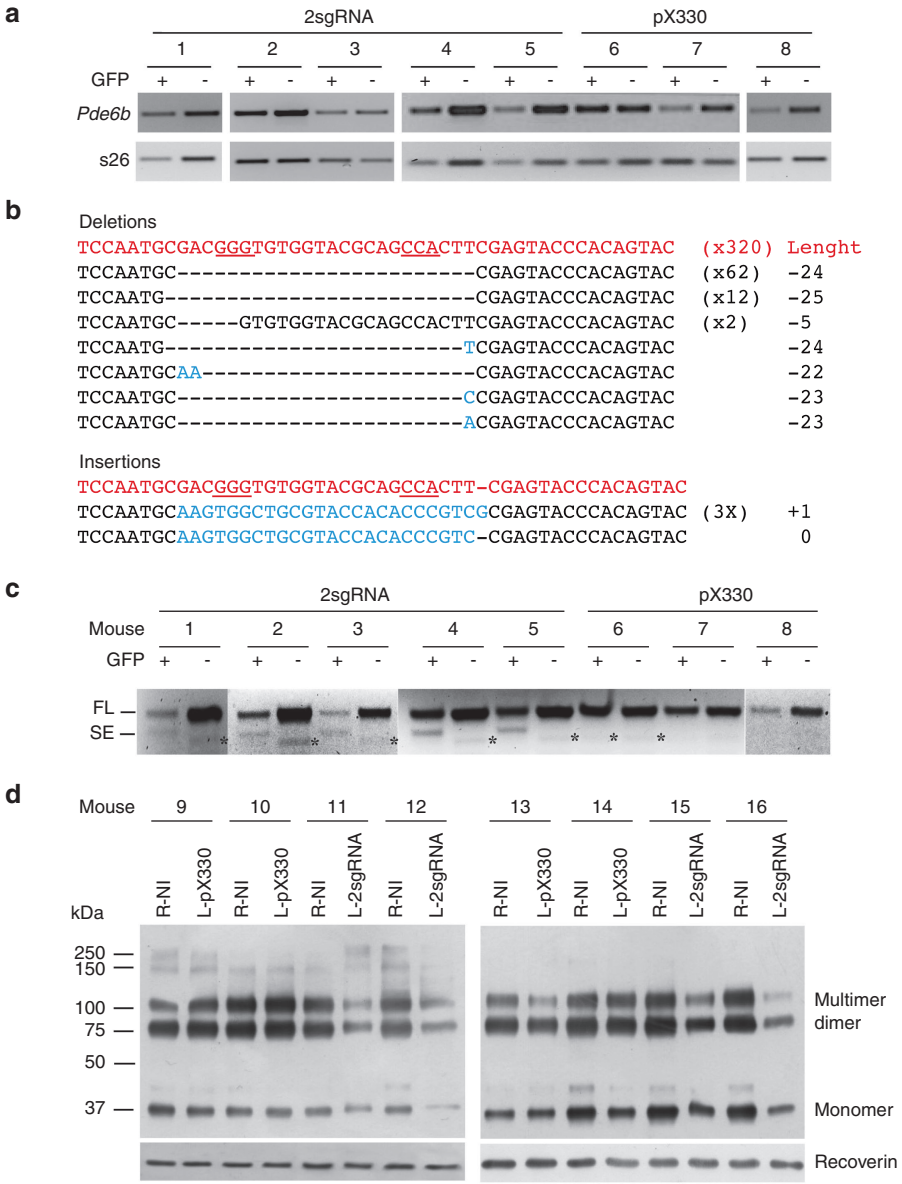

Figure 6 ***In vivo*** **knock-down of human P23H RHO in the retina.** (**a**) RT-PCR analysis of *Pde6b* expression in GFP⁺ and GFP⁻ cells sorted from mouse retinas electroporated with 2sgRNAs (#1–#5) or with pX330 (#6–#8). Ribosomal *s26* RNA was used for normalization. Similar expression of the rod photoreceptor specific gene *Pde6b* was observed in GFP⁺ and GFP⁻ sorted cells. (**b**) Sequences of PCR products surrounding the target sites amplified from the genomic DNA of GFP⁺ cells sorted from all mouse retinas injected with 2sgRNA. The top sequence in red is the unmodified sequence, underlined are the PAMs. The mismatches/insertions are indicated in cyan. The number of PCR amplicons for each sequence is reported in parentheses and the modified length is indicated. (**c**) End-point RT-PCR analysis on human *RHO* mRNA from GFP⁺ and GFP⁻ cells sorted from mouse retinas electroporated with 2sgRNAs (#1–#5), or with pX330 (#6–#8). FL indicates full-length P23H *RHO* transcript, SE indicates, short-edited transcript. Unspecific bands amplified in GFP⁻ cells from 2sgRNA or pX330 electroporated retinas are indicated by stars. (**d**) Immunoblot analysis of RHO on total protein extracts from GFP⁺ areas dissected as in **Figure 6a**. Four left 2sgRNA electroporated retinas (L-2sgRNA) were compared with the contralateral not-injected right retinas (R-NI) and showed reduction of RHO visible as monomer at 35 kDa and dimers/multimers at higher molecular weights. Four control left pX330 electroporated retinas (L-pX330) were compared with the contralateral not-injected right retinas (R-NI) and showed no significant change of RHO. The western blotting was normalized using antirecoverin antibodies, detecting a protein expressed in photoreceptors (lower panel).

2sgRNA-edited alleles, we observed the predominance (64%) of precise junctions between the two DSBs reflecting the described property of Cas9 to generate blunt ends 3 bp upstream of the PAM sequence.[36] P23H *RHO* knock-out was linked to a significant reduction of RHO expression *in vitro*. While the mRNA bearing the expected deletion upon 2sgRNA cleavage could be detected even if at low levels, the shorter RHO protein could not be distinguished with the resolution of the immunoblotting and notably we found a strong reduction of RHO protein that suggested instability of the protein, which was probably efficiently removed from the cell. Off-targets and cytotoxicity were addressed in P23H

Table 2 CRISPR/Cas9-mediated genome editing in transgenic P23H mice

Experiment	*Mouse*	*% Indels*		*% SE/FL RHO mRNA*		*% RHO protein reduction*	
		2sgRNA	w/o sgRNA	2sgRNA	w/o sgRNA	2sgRNA	w/o sgRNA
1	1	4		20		n.a	
	2	4		12		n.a	
	3	23		35		n.a	
	4	20		16		n.a	
	5	33		19		n.a	
2	17	33		n.a		n.a	
	18	33		n.a		n.a	
	19	19		n.a.		n.a	
3	20	n.d		n.a.		n.a	
	21	12		n.a.		n.a	
4	11	n.a.		n.a.		56	
	12	n.a.		n.a.		71	
	15	n.a.		n.a.		50	
	16	n.a.		n.a.		77	
5	6		n.d.		n.d.		n.a.
	7		n.d.		n.d.		n.a.
	8		n.d.		n.d.		n.a.
	22		n.d.		n.a.		n.a.
	23		n.d.		n.a.		n.a.
6	24		n.d.		n.a.		n.a.
7	9		n.a.		n.a.		n.d.
	10		n.a.		n.a.		n.d.
	13		n.a.		n.a.		n.d.
	14		n.a.		n.a.		n.d.

Fourteen mice in four different experiments (1–4) were injected with 2sgRNA. Genomic Indels were measured by Sanger sequencing of amplicons flanking the target site in the human *RHO* transgene in nine mice, not analyzed (n.a.) in four mice and not detected (n.d.) in one mouse. In the five-edited mice of the experiment 1 and in the four-edited mice of the experiment 4, we assessed the percentage of short-edited (SE) on the full-length (FL) RHO mRNA and the RHO protein reduction, respectively.About 10 mice in 3 different experiments (5–7) were injected with pX330 plasmid without sgRNA (w/o sgRNA). None of them showed Indels on the target sites, reduction in RHO expression at mRNA or protein level.

HeLa cells transfected with CRISPR/Cas9 system. We did not detect cleavage activity on the top 10 ranking off-target sites by Cell assay, able to detect mutations with frequencies ≥ 1%. To deeply address the off-target issue of sgRNAs with therapeutic relevance for a clinical application of the CRISPR/Cas9 system *in vivo*, a more appropriate method such as GUIDE-seq[37] should be performed. Alternatively, the therapeutic sgRNAs could be delivered together with the high fidelity SpCas9[38] which is reported to have even lower off-target cleavage events.

Most importantly, we demonstrated the feasibility of knocking-down the expression of mutated RHO *in vivo*, in the transgenic P23H mouse model. After retinal electroporation of the 2sgRNA the frequency of Indels reflected a lower knock-out efficiency than *in vitro* likely due to a lower copy number of Cas9-carrying plasmids delivered *in vivo* and to an already reported uncomparable genome editing efficiency *in vitro* versus *in vivo*.[39] However efficient knock-down in GFP^+ sorted cells was observed, and resulted in a significant reduction of mutant P23H protein. The different efficiencies scored in the analyses at distinct levels, *i.e.*, genomic, transcript, and protein, may be explained by the fact that not more than one analysis could be performed in the same animal due to the limited availability of the biological samples. Secondly, the sensitivities of the techniques are different and cannot be directly compared. Notably, reduction of human *RHO* transcript at similar levels (26%) was found sufficient to protect photoreceptor degeneration in the P347S mouse model.[9] Recently Botta *et al.*[10] reported 38% *RHO* transcriptional repression in the porcine retina followed by injection of an AAV8 vector carrying a *RHO*-specific DNA-binding repressor. Therefore, the levels of gene editing and mutant protein knock-down that we detected in the electroporated area of the retinas are in line with previous studies. Here we delivered the entire CRISPR/Cas9 system and sgRNAs using a single plasmid and, at the moment, the gene therapy delivery system in the clinic for the retina is based on AAV[40] that cannot accommodate the entire system but CRISPR/hSpCas9 components should be incorporated into two AAV8 vectors. This may improve delivery because AAV8 is very efficient for photoreceptor transduction but it may reduce genome editing due to the required coinfection by two viruses. This limitation may be overcome by the recently cloned *Cas9* genes from other species such as *N. meningitidis*[41] and *Staphylococcus aureus*[21,42,43] that are small enough to be efficiently packaged together with the sgRNAs into a single AAV8 vector.

This study demonstrates that CRISPR/Cas9 genome editing is a robust, easily programmable method to rapidly generate targeted frameshifts or genomic deletions in the retina.

Materials and methods

Plasmids. The pCCL-PGK.wtRHO and pCCL-PGK.P23H.RHO plasmids were generated by cloning the wtRHO.cDNA and P23H.RHO.cDNA (kindly provided by A. Auricchio) in pCCL.LV.PGK vector downstream PGK promoter.[44] The sgRNA1 and sgRNA3 plasmids were obtained by cloning the sgRNA1 and sgRNA3, respectively, in pX330 by oligo annealing into *Bbs*I sites (www.addgene.org). The 2sgRNA plasmid was achieved by cloning the U6-sgRNA3 into pX330-sgRNA1 downstream sgRNA1, in the same orientation. The pL.CRISPR-GFP.sgRNA1 and pL.CRISPR-GFP.sgRNA3 plasmids were generated by cloning sgRNA1 and sgRNA3, respectively, in pL.CRISPR-EFS.GFP (www.addgene.org) by oligo annealing into *Bsm*BI sites. The pL.CRISPR-GFP.2sgRNA was obtained by cloning the U6-sgRNA3 into pL.CRISPR-GFP.sgRNA1 downstream sgRNA1, in the same orientation.

Cell culture and viral production. HeLa and HEK293T cells were cultured in Dulbecco's modified Eagle's medium (DMEM) supplemented with 10% fetal calf serum (FCS), 100 U/ml penicillin and 100 mg/ml streptomycin (Lonza Ltd, Basel), Switzerland). Lentiviral stocks (LV) pseudotyped with the vesicular stomatitis virus G protein were prepared by transient cotransfection of HEK293T cells with transfer vector, pMD.Lg/pRRE.Int packaging plasmid, pMD2.VSV-G envelope–encoding plasmid, and pRSV-Rev.[45]

Transfections of HeLa cells, isolation of single cell clones, and VCN determination. Transfection 2.5×10^5 HeLa cells were transfected with Lipofectamine 3000 (ThermoFisher Scientific Monza, Italy). Each transfection reaction contains 2.5 ìg of DNA, 7.5 ìl of Lipofectamine 3000 and 5 ìl of Reagent P3000 and the mix was added to the cells accordingly to the manufacture's protocol.

Isolation of single cell clones. HeLa cells were transduced with LV for P23H *RHO* expression and the following day were limiting diluted to obtain a concentration of 0.3 cell/well in a 96 well plate. Genomic DNAs (gDNAs) extracted from single cell clones were screened by PCR on the RHO expression cassette as following: primers PGK.F and hRHO.1ex.R (**Supplementary Table S2**), PCR conditions: 30″ at 94°C, 30″ at 58°C, and 30″ at 72°C for 30 cycles. PCR products were separated on 1%TBE (Tris/Borate/EDTA)-agarose gels and stained with ethidium bromide for analysis.

VCN determination. qPCR was conducted with 20 ng gDNA in a 25 µl reaction using TaqMan Universal PCR Master Mix and probes specific for human RHO and glyceraldehyde 3-phosphate dehydrogenase (GAPDH) (hRHO: Hs00892431m1; GAPDH: Hs03929097_g1Applied Biosystem Milan, Italy). Reactions were performed at 50°C for 2 minutes and 95°C for 10 minutes, followed by 40 cycles at 95°C for 15 seconds and 60°C for 1 minute. The relative copy number was normalized to the GAPDH in the same gDNA by using the $2^{-\Delta\Delta CT}$ quantification.

Immunofluorescence on HeLa clones. Cells were fixed with 4% paraformaldehyde in phosphate buffered saline (PBS) for 10 minutes. For colocalization analysis fixed cells were permeabilized and blocked in PBS with 3% bovine serum albumin (BSA) and 0.1% TritonX-100 for 1 hour at room temperature, washed five times with PBS and incubated with the monoclonal mouse anti-RHO antibody 1D4 (epitope at the C-terminal of RHO; R5403, Sigma Aldrich, Milan, Italy; 1:1,000) together with the polyclonal rabbit anticalnexin antibody (H-70: sc-11397, Santa Cruz Biotechnology Heidelberg, Germany; 1:50) overnight at 4°C. To analyze the membrane localization of RHO, fixed cells were blocked in PBS with 3% BSA without detergent to avoid permeabilization of the cell membrane and incubated with the primary mouse anti-RHO antibody RetP1 (epitope at the N-terminal of RHO; ab3267 Abcam Cambridge, UK; 1:10,000). As secondary antibodies we used Alexa Flour 568 goat antirabbit and Oregon-Green 488 goat antimouse (Invitrogen Milan, Italy; 1:1,000) incubated with 0.1 µg/ml 4′,6-diamidino-2-phenylindole (DAPI) for nuclear staining. Slides were mounted with Mowiol 4–88 (Sigma Aldrich) and analyzed with a Zeiss Axioskop 40 FL fluorescence microscope equipped with a digital camera AxioCam and AxioVisionRel version 4.8 software for image processing (Zeiss Oberkochen, Germany). Colocalization of the 1D4 and CLNX immunofluorescence was evaluated by calculating the PCC which determines the relative fluorescence intensities of the green Oregon-Green 488 (labeling RHO) and red Alexa Flour 568 (labeling calnexin) in the same groups of pixels in a region of interest.[28] The channels of single RGB images were split into grayscale pictures and the red and green channels used for analysis. A region of interest in the green channel was created by free hand drawing around the RHO fluorescence in single cells and used for calculating PCC (see[28] for details). PCC values can range from +1 to –1. Whereas a value of 1 represents perfect correlation (protein retained into the ER), value –1 represents perfect but inverted correlation and values near zero represent distributions of fluorescent signals that are uncorrelated with one another.[28] The mean PCC-values derived from five cells for each clone were used for statistical analysis by Student's unpaired *t*-test. All data are presented as mean values ± standard errors of the means (SEMs).

Surveyor assay and DNA sequence analysis. For the Cel-I nuclease assay to detect CRISPR/Cas9-mediated mutations, the SURVEYOR Mutation Detection Kit (Transgenomic, Omaha, NE) was used in accordance with the manufacturer's protocol. Briefly, 48 hours after transfection, genomic DNA was extracted using the DNeasy MiniKit (QIAGEN Hilden, Germany). PCR to detect the on target cleavage was performed with the primers PGK.F, and hRHO.1ex.R (**Supplementary Table S2**). To amplify the off targets predicted by a public webserver (http://crispr.mit.edu), we designed several primers listed in **Supplementary Table S2**. The amplification products were denatured and digested by the Cel-I nuclease, and then subjected to 2% agarose gel electrophoresis for on-targets and off-targets. For DNA sequence analysis of the on target Indels, the PCR products were subcloned into a PCR2.1 TOPO vector (ThermoFisher Scientific) and Sanger sequenced (Eurofin s.r.l Vimodrone, Italy).

Semiquantitative and quantitative RT-PCR analyses. Total RNA from HeLa cells was isolated with the RNeasy Mini kit

plus (Qiagen, Hilden, Germany), according to the manufacturer's protocol. cDNA was synthesized in a 20 µl reaction using 500 ng total RNA and SuperScript III (Life Technologies Monza, Italy). Total RNAs from GFP$^+$ and GFP$^-$ FACS-sorted cells were extracted using the QIAGEN RNeasy Micro Kit (Qiagen Hilden, Germany), according to the manufacturer's protocol. cDNA was synthesized in a 20 µl reaction using all total RNA purified from GFP$^+$ sorted cells and SuperScript III (Life Technologies).

Semiquantitative RT-PCR analyses were performed with the following oligonucleotides:

- PGK.F2 and hRHO.ex1.R2, GAPDH.F and GAPDH.R for mRNA analysis of HeLa cells
- Cas9.F and Cas9.R and GFP.F and GFP.R for mRNA analysis of electroporated and not electroporated retina
- hRho.5UTR.F and hRho.ex1.R2, m.s26rRNA.F and m.s26rRNA.R, PDE6b.F and PDE6b.R for mRNA analysis of GFP$^+$ and GFP$^-$ FACS-sorted cells from electroporated retinas.

PCR cycles. 94°C 30 seconds, 58°C 30 seconds, and 72°C 30 seconds.

Quantitative RT-PCR analysis. TaqMan RT-PCR analysis was performed with ABI Prism 7900 Sequence Detection System (Applied Biosystems Monza, Italy) with TaqMan Universal PCR Master Mix and probes specific for human RHO and GAPDH (hRHO: Hs00892431m1; GAPDH: NM_02046.3 Applied Biosystem Monza, Italy). Reactions were performed at 50°C for 2 minutes and 95°C for 10 minutes, followed by 40 cycles at 95°C for 15 seconds and 60°C for 1 minute. The relative expression of the target genes was normalized to the level of GAPDH in the same cDNA by using the $2^{-\Delta\Delta CT}$ quantification. The replicated Relative Quantity (RQ) values for each biological sample were averaged.

Apoptosis analysis. PE Annexin V Apoptosis Detection Kit I (BD Pharmigen Milan, Italy) was used according to manufacturer's protocol to measure apoptosis. Briefly, 72 hours post-transfection cells were washed twice with cold PBS and resuspended in 1X Annexin V Binding Buffer at a concentration of 1×10^6 cells/ml. 1×10^5 cells were stained with 5 µl of PE-Annexin V and 5 µl 7-Amino-Actinomycin (7-AAD) for 15 minutes at RT (25°C) in the dark. After incubation, 400 µl of 1X Annexin V Binding Buffer were added to each tube. Fluorescence was acquired within 1 hour on a FACS CANTO cytofluorimeter (BD Biosciences Milan, Italy). Annexin V is a calcium-dependent phospholipid-binding protein with high affinity for phosphatidylserine exposed on apoptotic cell membrane. The flow cytometric viability probe 7-AAD only permeates membranes of dead and damaged cells, thus is useful to distinguish viable from nonviable cells. Cells undergoing apoptosis are PE-Annexin V positive/7-AAD negative. Cells in the end stage of apoptosis, undergoing necrosis, or already dead are PE-Annexin V positive/7-AAD positive. Live cells are PE-Annexin V negative/7-AAD negative and not undergoing measurable apoptosis.

Statistical analysis. Data were analyzed for statistical significance using two-way ANOVA or Student's *t*-test. All values in each group were expressed as the mean ± SEM. All group comparisons were considered significant at $P < 0.05$, $P < 0.01$, $P < 0.001$.

Animal care and electroporation. All procedures on mice were conducted at CSSI (Centro Servizi Stabulario Interdipartimentale) and approved by the Ethical Committee of University of Modena and Reggio Emilia (Prot. N. 106 22/11/2012) and by Italian Ministero della Salute (346/2015-PR). RHO P23H transgenic mice (P23H^{Tg})[29] were housed in a 12- hour light/dark cycle, had free access to food and water and were used irrespective of gender. P23H^{Tg} were bred to Rho$^{-/-}$ mice,[30] kindly provided by Humphries, to generate mice expressing only the human P23H-RHO (Rho$^{-/-}$P23H^{Tg}). This knock-out does not express murine Rho although the first exon is intact and could, potentially, be recognized by the designed sgRNAs. All mice were genotyped as previously published.[29,30] The pX330 or 2sgRNA, together with the plasmid pCAG-GFP expressing GFP, were electroporated in Rho$^{-/-}$P23H^{Tg} neonatal mice as previously published.[31,32] In brief, newborn murine pups were anesthetized by chilling on ice and eyelids were opened using a scalpel. After piercing the sclera with a 30-gauge needle, 0.5 µl of DNA solution (6 mg/ml) was delivered subretinally by using a Hamilton syringe. After DNA injection five 90 V square pulses of 50 milliseconds duration were applied with a T820 electroporation system (BTX, San Diego California, USA). Electroporated retinas were harvested 7 days after electroporation and electroporated areas were dissected under a Leica fluorescent stereoscope and proteins extracted for western blotting analysis. For genomic and mRNA analyses the entire electroporated retinas were treated in papain (0.6 U in 30 µl) for 30 minutes, the enzyme was diluted 33 times with DMEM in the presence of DNAse (12.5 U) and cells dissociated by trituration with a Gilson pipet. After washing with DMEM, dissociated retina cells were sorted at 488 nm based on GFP expression by FACS (BD FACSAriaIII Cell Sorter Milan, Italy).

Retinal protein extracts and western blotting analysis. Retinas were dissected in PBS. Tissue was disrupted in lysis buffer (PBS, 17 mmol/l CHAPS, protease inhibitor cocktail from Sigma) for 30 minutes at 4°C. After centrifugation at 17,400×*g* for 30 minutes the supernatant was collected.

Equivalent amounts of protein extracts (30 µg for HeLa cells, 5 µg for analyses of transgenic human RHO in the retina and 10 ng for wild type murine Rho in the retina) were resolved using sodium dodecyl sulfate (SDS)-polyacrylamide gel electrophoresis (PAGE) and immunoblotting was performed following standard procedures. The antibodies used were: anti-RHO (1D4, recognizing an epitope at the C-term, 1:10,000; Sigma), antirecoverin (1:2,000, Millipore), anti-α-tubulin (1:2,500, Sigma). Quantification was performed by densitometry analysis of scanned images using Image J software, corrected by background, and plotted as protein levels of RHO over the reference protein. Data are mean ± SD of three blots with proteins derived from four animals from two biological replicates.

Supplementary material

Figure S1. Schematic representation of pX330 and pX330-derived plasmids carrying Cas9 and one or more gRNAs.

Figure S2. qPCR on P23H RHO and wt RHO.
Figure S3. Expression of RHO in stable HeLa clones.
Figure S4. Generation of an *in vitro* model carrying the P23H RHO mutation.
Figure S5. Localization of WT RHO in stable clones.
Figure S6. Quantitative expression of P23H *Rhodopsin* in clone #80 respect to the clone #78.
Figure S7. Flow cytometry analysis of cell toxicity induced by the CRISPR/Cas9 system.
Figure S8. Indel spectrum determined by TIDE analysis on human *RHO* gene in the GFP- fraction of mouse retinas treated with 2sgRNA.
Figure S9. Indel spectrum determined by TIDE analysis on human *RHO* gene in the GFP+ fraction of mouse retinas treated with pX330.
Figure S10. Indel spectrum determined by TIDE analysis on mouse *Rho* gene in the GFP+ fraction of mouse retinas treated with 2sgRNA.
Figure S11. Densitometry analysis of short edited respect to the full length mRNA RHO in the GFP+ cells from 2sgRNA-electroporated retinas.
Figure S12. Densitometry analysis and scatter plot of RHO protein levels.
Table S1. Predicted off-targets for sgRNA1 and sgRNA3.
Table S2. Primers used in this study.

Acknowledgments This work has been supported by AFM Telethon project 16663, Programma Strategico RARER-Programma di ricerca Regione-Università 2010–2012, Fondazione Roma (call for proposal 2013 sulla Retinite Pigmentosa). The authors acknowledge the CSSI of University of Modena and Reggio Emilia for providing animal husbandry assistance.

1. Lefkowitz, RJ (2007). Seven transmembrane receptors: something old, something new. *Acta Physiol (Oxf)* **190**: 9–19.
2. Conn, PM and Ulloa-Aguirre, A (2010). Trafficking of G-protein-coupled receptors to the plasma membrane: insights for pharmacoperone drugs. *Trends Endocrinol Metab* **21**: 190–197.
3. Hartong, DT, Berson, EL and Dryja, TP (2006). Retinitis pigmentosa. *Lancet* **368**: 1795–1809.
4. Krebs, MP, Holden, DC, Joshi, P, Clark, CL 3rd, Lee, AH and Kaushal, S (2010). Molecular mechanisms of rhodopsin retinitis pigmentosa and the efficacy of pharmacological rescue. *J Mol Biol* **395**: 1063–1078.
5. Comitato, A, Sanges, D, Rossi, A, Humphries, MM and Marigo, V (2014). Activation of Bax in three models of retinitis pigmentosa. *Invest Ophthalmol Vis Sci* **55**: 3555–3562.
6. Kunte, MM, Choudhury, S, Manheim, JF, Shinde, VM, Miura, M, Chiodo, VA *et al.* (2012). ER stress is involved in T17M rhodopsin-induced retinal degeneration. *Invest Ophthalmol Vis Sci* **53**: 3792–3800.
7. Sakami, S, Kolesnikov, AV, Kefalov, VJ and Palczewski, K (2014). P23H opsin knock-in mice reveal a novel step in retinal rod disc morphogenesis. *Hum Mol Genet* **23**: 1723–1741.
8. Comitato, A, Di Salvo, MT, Turchiano, G, Montanari, M, Sakami, S, Palczewski, K *et al.* (2016). Dominant and recessive mutations in rhodopsin activate different cell death pathways. *Hum Mol Genet* (epub ahead of print).
9. Mussolino, C, Sanges, D, Marrocco, E, Bonetti, C, Di Vicino, U, Marigo, V *et al.* (2011). Zinc-finger-based transcriptional repression of rhodopsin in a model of dominant retinitis pigmentosa. *EMBO Mol Med* **3**: 118–128.
10. Botta, S, Marrocco, E, de Prisco, N, Curion, F, Renda, M, Sofia, M *et al.* (2016). Rhodopsin targeted transcriptional silencing by DNA-binding. *Elife* **5**: e12242.
11. Millington-Ward, S, Chadderton, N, O'Reilly, M, Palfi, A, Goldmann, T, Kilty, C *et al.* (2011). Suppression and replacement gene therapy for autosomal dominant disease in a murine model of dominant retinitis pigmentosa. *Mol Ther* **19**: 642–649.
12. Hsu, PD, Lander, ES and Zhang, F (2014). Development and applications of CRISPR-Cas9 for genome engineering. *Cell* **157**: 1262–1278.
13. Jinek, M, Chylinski, K, Fonfara, I, Hauer, M, Doudna, JA and Charpentier, E (2012). A programmable dual-RNA-guided DNA endonuclease in adaptive bacterial immunity. *Science* **337**: 816–821.
14. Li, JF, Norville, JE, Aach, J, McCormack, M, Zhang, D, Bush, J *et al.* (2013). Multiplex and homologous recombination-mediated genome editing in Arabidopsis and Nicotiana benthamiana using guide RNA and Cas9. *Nat Biotechnol* **31**: 688–691.
15. Hwang, WY, Fu, Y, Reyon, D, Maeder, ML, Tsai, SQ, Sander, JD *et al.* (2013). Efficient genome editing in zebrafish using a CRISPR-Cas system. *Nat Biotechnol* **31**: 227–229.
16. Bassett, AR, Tibbit, C, Ponting, CP and Liu, JL (2013). Highly efficient targeted mutagenesis of Drosophila with the CRISPR/Cas9 system. *Cell Rep* **4**: 220–228.
17. Wang, H, Yang, H, Shivalila, CS, Dawlaty, MM, Cheng, AW, Zhang, F *et al.* (2013). One-step generation of mice carrying mutations in multiple genes by CRISPR/Cas-mediated genome engineering. *Cell* **153**: 910–918.
18. Niu, Y, Shen, B, Cui, Y, Chen, Y, Wang, J, Wang, L *et al.* (2014). Generation of gene-modified cynomolgus monkey via Cas9/RNA-mediated gene targeting in one-cell embryos. *Cell* **156**: 836–843.
19. Mali, P, Yang, L, Esvelt, KM, Aach, J, Guell, M, DiCarlo, JE *et al.* (2013). RNA-guided human genome engineering via Cas9. *Science* **339**: 823–826.
20. Cho, SW, Kim, S, Kim, JM and Kim, JS (2013). Targeted genome engineering in human cells with the Cas9 RNA-guided endonuclease. *Nat Biotechnol* **31**: 230–232.
21. Ran, FA, Cong, L, Yan, WX, Scott, DA, Gootenberg, JS, Kriz, AJ *et al.* (2015). *In vivo* genome editing using Staphylococcus aureus Cas9. *Nature* **520**: 186–191.
22. Ousterout, DG, Kabadi, AM, Thakore, PI, Majoros, WH, Reddy, TE and Gersbach, CA (2015). Multiplex CRISPR/Cas9-based genome editing for correction of dystrophin mutations that cause Duchenne muscular dystrophy. *Nat Commun* **6**: 6244.
23. Rossmiller, B, Mao, H and Lewin, AS (2012). Gene therapy in animal models of autosomal dominant retinitis pigmentosa. *Mol Vis* **18**: 2479–2496.
24. Cong, L, Ran, FA, Cox, D, Lin, S, Barretto, R, Habib, N *et al.* (2013). Multiplex genome engineering using CRISPR/Cas systems. *Science* **339**: 819–823.
25. Saliba, RS, Munro, PM, Luthert, PJ and Cheetham, ME (2002). The cellular fate of mutant rhodopsin: quality control, degradation and aggresome formation. *J Cell Sci* **115**(Pt 14): 2907–2918.
26. Chiang, WC, Messah, C and Lin, JH (2012). IRE1 directs proteasomal and lysosomal degradation of misfolded rhodopsin. *Mol Biol Cell* **23**: 758–770.
27. Kosmaoglou, M and Cheetham, ME (2008). Calnexin is not essential for mammalian rod opsin biogenesis. *Mol Vis* **14**: 2466–2474.
28. Dunn, KW, Kamocka, MM and McDonald, JH (2011). A practical guide to evaluating colocalization in biological microscopy. *Am J Physiol Cell Physiol* **300**: C723–C742.
29. Olsson, JE, Gordon, JW, Pawlyk, BS, Roof, D, Hayes, A, Molday, RS *et al.* (1992). Transgenic mice with a rhodopsin mutation (Pro23His): a mouse model of autosomal dominant retinitis pigmentosa. *Neuron* **9**: 815–830.
30. Humphries, MM, Rancourt, D, Farrar, GJ, Kenna, P, Hazel, M, Bush, RA *et al.* (1997). Retinopathy induced in mice by targeted disruption of the rhodopsin gene. *Nat Genet* **15**: 216–219.
31. Comitato, A, Spampanato, C, Chakarova, C, Sanges, D, Bhattacharya, SS and Marigo, V (2007). Mutations in splicing factor PRPF3, causing retinal degeneration, form detrimental aggregates in photoreceptor cells. *Hum Mol Genet* **16**: 1699–1707.
32. Matsuda, T, and Cepko, CL (2004). Electroporation and RNA interference in the rodent retina *in vivo* and *in vitro*. *Proc Natl Acad Sci USA* **101**: 16–22.
33. Dryja, TP, McGee, TL, Reichel, E, Hahn, LB, Cowley, GS, Yandell, DW *et al.* (1990). A point mutation of the rhodopsin gene in one form of retinitis pigmentosa. *Nature* **343**: 364–366.
34. Bakondi, B, Lv, W, Lu, B, Jones, MK, Tsai, Y, Kim, KJ *et al.* (2016). *In vivo* CRISPR/Cas9 gene editing corrects retinal dystrophy in the S334ter-3 rat model of autosomal dominant retinitis pigmentosa. *Mol Ther* **24**: 556–563.
35. Chan, F, Hauswirth, WW, Wensel, TG and Wilson, JH (2011). Efficient mutagenesis of the rhodopsin gene in rod photoreceptor neurons in mice. *Nucleic Acids Res* **39**: 5955–5966.
36. Cheong, TC, Compagno, M and Chiarle, R (2016). Editing of mouse and human immunoglobulin genes by CRISPR-Cas9 system. *Nat Commun* **7**: 10934.
37. Zhang, XH, Tee, LY, Wang, XG, Huang, QS and Yang, SH (2015). Off-target effects in CRISPR/Cas9-mediated genome engineering. *Mol Ther Nucleic Acids* **4**: e264.
38. Kleinstiver, BP, Pattanayak, V, Prew, MS, Tsai, SQ, Nguyen, NT, Zheng, Z *et al.* (2016). High-fidelity CRISPR-Cas9 nucleases with no detectable genome-wide off-target effects. *Nature* **529**: 490–495.
39. Tabebordbar, M, Zhu, K, Cheng, JK, Chew, WL, Widrick, JJ, Yan, WX *et al.* (2016). *In vivo* gene editing in dystrophic mouse muscle and muscle stem cells. *Science* **351**: 407–411.
40. Maguire, AM, Simonelli, F, Pierce, EA, Pugh, EN Jr, Mingozzi, F, Bennicelli, J *et al.* (2008). Safety and efficacy of gene transfer for Leber's congenital amaurosis. *N Engl J Med* **358**: 2240–2248.
41. Hou, Z, Zhang, Y, Propson, NE, Howden, SE, Chu, LF, Sontheimer, EJ, *et al.* (2013). Efficient genome engineering in human pluripotent stem cells using Cas9 from Neisseria meningitidis. *Proc Natll Acad Sci USA* **110**: 15644–15649.

42. Friedland, AE, Baral, R, Singhal, P, Loveluck, K, Shen, S, Sanchez, M *et al.* (2015). Characterization of Staphylococcus aureus Cas9: a smaller Cas9 for all-in-one adeno-associated virus delivery and paired nickase applications. *Genome Biol* **16**: 257.
43. Kleinstiver, BP, Prew, MS, Tsai, SQ, Nguyen, NT, Topkar, VV, Zheng, Z *et al.* (2015). Broadening the targeting range of Staphylococcus aureus CRISPR-Cas9 by modifying PAM recognition. *Nat Biotechnol* **33**: 1293–1298.
44. Coluccio, A, Miselli, F, Lombardo, A, Marconi, A, Malagoli Tagliazucchi, G, Gonçalves, MA *et al.* (2013). Targeted gene addition in human epithelial stem cells by zinc-finger nuclease-mediated homologous recombination. *Mol Ther* **21**: 1695–1704.
45. Dull, T, Zufferey, R, Kelly, M, Mandel, RJ, Nguyen, M, Trono, D *et al.* (1998). A third-generation lentivirus vector with a conditional packaging system. *J Virol* **72**: 8463–8471.

Supplementary Information accompanies this paper on the Molecular Therapy–Nucleic Acids website (http://www.nature.com/mtna)